

Figure 1. Scope of metal-catalyzed amination of aryl sulfamates.

nucleophiles, including anilines, primary and secondary alkyl amines, heteroaryl amines, *N*-heterocycles, and primary amides (Figure 1B). In addition, we provide evidence by DFT calculation that in the polar protic medium, a cationic pathway is operating.

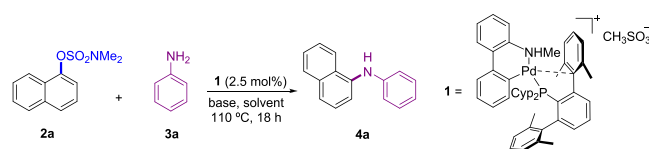
RESULTS AND DISCUSSION

In a previous work, we described the catalytic capability of a cationic *N*-methyl-2-aminobiphenyl palladacycle supported by sterically demanding phosphine PCyp₂Ar^{Xyl2}, **1**, in the amination of aryl chlorides.^{11b} The advantage of this precatalyst over the parent 2-aminobiphenyl palladacycle is that its activation in the presence of the base releases *N*-methyl carbazole, a byproduct that cannot hinder the catalytic reaction.¹³

Using precatalyst **1** (2.5 mol %), we examined the coupling of naphthalen-1-yl dimethylsulfamate with aniline applying the reaction conditions developed for the amination of aryl chlorides,^{11b} namely, NaOtBu, as the base, dioxane as the solvent, and 110 °C as the reaction temperature. Under these conditions, a promising conversion to the expected *N*-phenylnaphthalen-1-amine, **4a**, of 27% was observed by GC analysis (Table 1, entry 1). To further improve the yield, different solvents were investigated (entries 2–5). Either toluene or DMF provided lower conversions. The use of a protic solvent, such as *t*BuOH, which has been successfully applied in Pd-catalyzed C–N couplings,¹⁴ also resulted in lower yield of the product. It has been found that the addition of water can enhance the rate of the amination.^{14b,15} To our delight, the use of a 8:1 (vol.) mixture of *t*BuOH:H₂O significantly increased the conversion, but for driving the reaction to completion, a 1:1 mixture of *t*BuOH and water was crucial, product **4a** being isolated in 97% yield (entries 6–8; see also Table S1). Lowering the catalyst loading or using bases other than NaOtBu reduced the reaction efficiency (entries 9–11); in the latter case, decomposition of the naphthyl sulfamate into naphthol was observed. Notably, complete conversion was also achieved at temperatures as low as 60 °C (entry 12), and even at room temperature, **1** proved to be reactive giving product **4a** in 74% yield (entry 13). However, a reaction temperature of 110 °C was used to study the reaction scope to accomplish the coupling of more challenging substrates.

Using the optimized reaction conditions, we tested other ligands using the corresponding ligated *N*-methyl-2-aminobiphenyl palladacycles (see Table S2). Only with XPhos-

Table 1. Screening of Conditions for the Coupling of Naphthalen-1-yl Dimethylsulfamate and Aniline^a



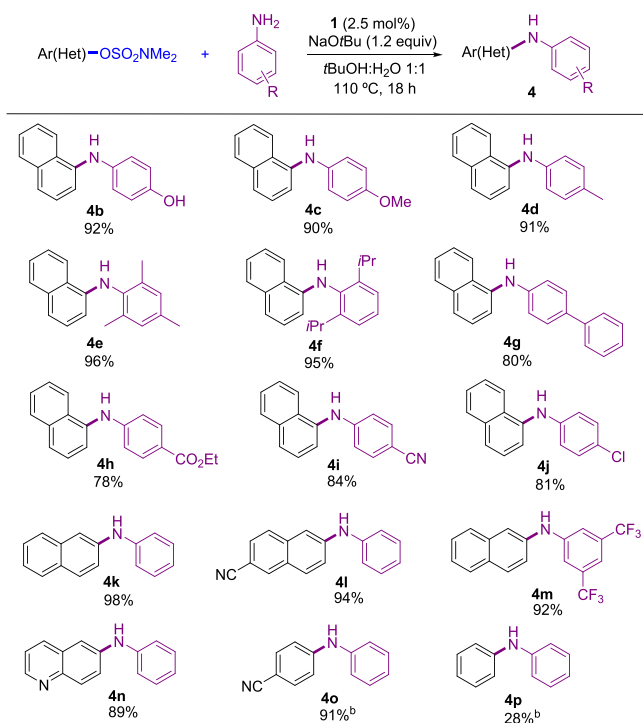
entry	base	solvent	conversion ^b (%)
1	NaOtBu	dioxane	27
2	NaOtBu	THF	12
3	NaOtBu	toluene	9
4	NaOtBu	DMF	15
5	NaOtBu	<i>t</i> BuOH	4
6	NaOtBu	<i>t</i> BuOH:H ₂ O (8:1)	43
7	NaOtBu	<i>t</i> BuOH:H ₂ O (3:1)	94
8	NaOtBu	<i>t</i> BuOH:H ₂ O (1:1)	100 (97) ^c
9 ^d	NaOtBu	<i>t</i> BuOH:H ₂ O (1:1)	90 (85) ^c
10	LiOtBu	<i>t</i> BuOH:H ₂ O (1:1)	99 (91) ^c
11	NaOH	<i>t</i> BuOH:H ₂ O (1:1)	100 (90) ^c
12 ^e	NaOtBu	<i>t</i> BuOH:H ₂ O (1:1)	100 (92) ^c
13 ^f	NaOtBu	<i>t</i> BuOH:H ₂ O (1:1)	(74) ^c

^aReaction conditions: naphthyl sulfamate (**1** mmol), amine (1.2 mmol), base (1.2 mmol), **1** (0.025 mmol), solvent (2 mL), *T* = 110 °C, 18 h (unoptimized). ^bConversion estimated by GC analysis of the reaction mixtures. ^cYields of isolated products (average of two runs). ^d**1** (0.020 mmol). ^e*T* = 60 °C. ^fReaction performed at room temperature.

supported palladacycle was the conversion comparable to that obtained with our precatalyst. However, precatalyst **1** outperformed the catalytic abilities of the XPhos-supported precatalyst when we examined the amination of other substrate combinations (see Table S3).

Under the optimized conditions, we examined the coupling of a variety of aryl sulfamates and anilines. As shown in Scheme 1, sulfamates derived from 1- and 2-naphthol could be successfully employed as reactant partners in this transformation (**4b–4m**). Furthermore, the catalytic system tolerated a quinoline core in the electrophile (**4n**). The nonfused ring *p*-cyanophenyl sulfamate could be efficiently coupled with aniline (**4o**); however, poor results were obtained with the less reactive phenyl sulfamate (**4p**; see Table S4). Regarding the aniline, the scope was broad. Both, electron-rich and electron-poor anilines provided the corresponding coupling products in yields higher than 81% (**4b–4j**, **4m**). Moreover, *ortho*-substituted anilines were arylated in excellent yields (**4e**, **4f**). Interestingly, naphthyl sulfamates could be selectively coupled with anilines bearing chloride (**4j**) or free hydroxyl functionalities (**4b**), avoiding the need of protecting groups or the use of weaker bases in the latter case.

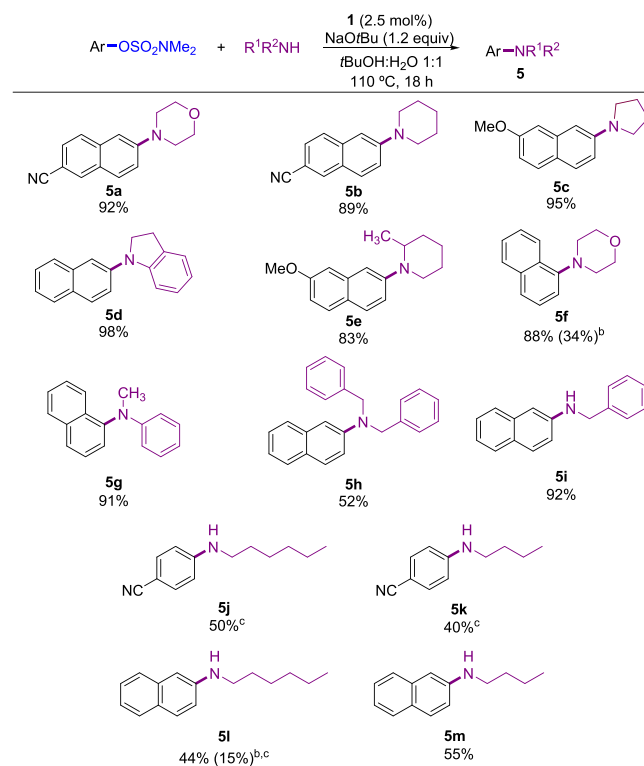
Next, the scope of aliphatic amines was explored (Scheme 2). Both cyclic and acyclic secondary amines proved to be suitable substrates furnishing the arylated products in useful synthetic yields, using the optimized reaction conditions (Scheme 2, **5a–h**). Primary aliphatic amines have not been previously tested in Ni-catalyzed amination of aryl sulfamates. We found that our catalyst system enabled the coupling of benzylamine with naphthalen-2-yl sulfamate in high yield (**5i**). Moreover, linear alkyl primary amines could also be arylated with both naphthyl and phenyl-derived sulfamates, albeit in moderate yield (**5j–5m**).

Scheme 1. Pd-Catalyzed *N*-Arylation of Anilines with Aryl Sulfamates^a

^aReaction conditions: aryl sulfamate (1.0 mmol), amine (1.2 mmol), NaOtBu (1.2 mmol), **1** (0.025 mmol), solvent (2 mL), 110 °C, 18 h. Isolated yields of pure products. ^bReaction performed with 3 mol % catalyst loading.

In light of the reactivity displayed by precatalyst **1** toward amines, we focused on more challenging *N*-nucleophiles like heteroarylamines and *N*-heterocycles, since they are present as substructures in biologically active molecules, natural products, and pharmaceuticals.^{12a,16} An array of substrate combinations were screened under the optimized conditions (Scheme 3). Regarding the heteroarylamines, 2- and 3-aminopyridine, 2-aminopyrimidine, and 2-aminopyrazine were successfully arylated providing the corresponding diarylamines in isolated yields ranging from 44 to 97% (Scheme 3, 6a–f). 2-Aminooxazol and 2-aminobenzoxazol were efficiently coupled with electron-rich and electron-deficient naphthyl sulfamate derivatives (**6g**, **6h**). Pyridine methanamines were found compatible with the catalyst system, affording the *N*-arylated heterocycles in high yields (**6i**, **6j**). Moreover, *N*-heterocycles such as pyrrole, pyrazole, and carbazole reacted with naphthalen-2-yl sulfamate, giving the desired cross-coupling products in moderate to high yields (Scheme 3, 7a–7c). Chemoselective *N*-arylation of indoles was efficiently accomplished (**7d–f**, **7h**) although, with more hindered 2-substituted indoles, slightly lower yields were obtained (**7g**, **7i**, **7j**). To our knowledge, these results represent the first use of aryl sulfamates as electrophiles in the amination of a variety of *N*-nucleophiles that are relevant in pharmaceutical synthesis.

Amides are problematic substrates in Pd-catalyzed C–N cross-coupling reactions, due to their reduced nucleophilicity together with their tendency to form *k*²-amidate complexes, responsible for retarding the rate of the reductive elimination step.¹⁷ However, despite these shortcomings, Pd-based catalysts have been developed that enable the *N*-arylation of amides even with C–O electrophiles,^{14b,18} albeit limited to the

Scheme 2. Pd-Catalyzed *N*-Arylation of Aliphatic Amines with Aryl Sulfamates^a

^aReaction conditions: aryl sulfamate (1.0 mmol), amine (1.2 mmol), NaOtBu (1.2 mmol), **1** (0.025 mmol), solvent (2 mL), 110 °C, 18 h. Isolated yields of pure products. ^bConversion obtained using the Pd-XPhos precatalyst (Table S3). ^c4 mol % **1**.

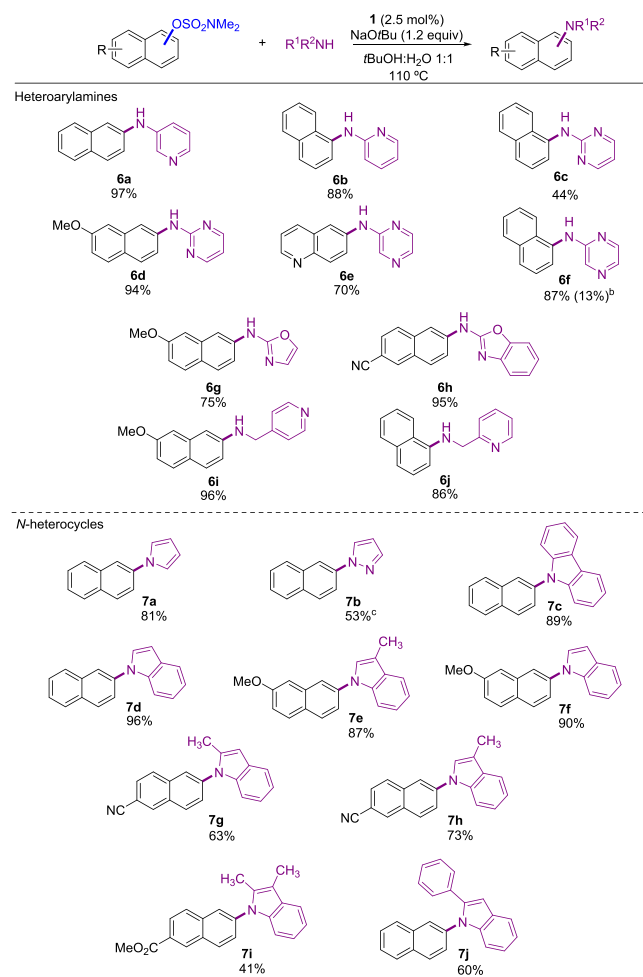
more reactive aryl sulfonates. We were pleased to find that parent benzamide and electron-rich and electron-poor benzamide derivatives were all effective *N*-arylated using the disclosed protocol (Scheme 4, 8a–d).

Formamide proved to be more difficult resulting in modest yield of the desired product (**8e**). We are aware of a single example in which an aryl sulfamate was used as electrophile in a Ni-catalyzed *N*-arylation of primary amides.¹⁹

The catalytic cycle for the aryl amination reactions is well established²⁰ and involves the three main steps common to any cross-coupling catalytic manifold: the oxidative addition, the ligand exchange (amine coordination and deprotonation), and the reductive elimination. Almost all the computational studies on C–N coupling reactions have been carried out with aryl halides as model electrophiles. To our knowledge, there is only one theoretical report, focused on the role of DBU as a base in C–N couplings with Pd/phosphine catalysts, in which a phenol-derived electrophile, *p*-tolyl triflate, is considered in the calculations.^{20h} Bearing this in mind, we decided to explore the mechanism of the amination of aryl sulfamates with DFT calculations using (PCyp₂Ar^{Xyl2})Pd(0) as the catalyst, naphthalen-1-yl dimethylsulfamate and aniline as the substrates, *t*BuO[−] and OH[−] as bases, and ethanol as the solvent, for the model chemical system. We used density functional methods (M06L/6-31g(d,p)/SDD//M06/6-311+g(2d,p)/LANL2TZ-(f)).

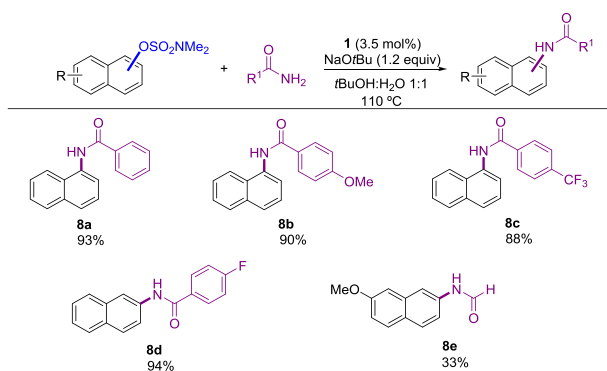
We have shown that terphenyl phosphines can adopt pseudobidentate coordination modes, providing additional stabilization by noncovalent interactions between the metal

Scheme 3. Pd-Catalyzed *N*-Arylation of Heteroarylamines and *N*-Heterocycles with Aryl Sulfamates^a



^aReaction conditions: aryl sulfamate (1.0 mmol), amine (1.2 mmol), NaOtBu (1.2 mmol), **1** (0.025 mmol), solvent (2 mL), 110 °C, 18 h. Isolated yields of pure products. ^bConversion obtained using the Pd-XPhos precatalyst (Table S3). ^c5 mol % **1**.

Scheme 4. Pd-Catalyzed *N*-Arylation of Amides with Aryl Sulfamates^a



^aReaction conditions: aryl sulfamate (1.0 mmol), amine (1.2 mmol), NaOtBu (1.2 mmol), **1** (0.035), solvent (2 mL), 110 °C, 18 h. Isolated yields of pure products.

center and a side ring of the terphenyl moiety.^{9a,10} Our calculations account for an extra stabilization of ca. -12 kcal mol⁻¹ in ethanol for the PCyp₂Ar^{Xyl2}-ligated Pd(0) active

species when the phosphine is binding in a pseudobidentate fashion (see Figure S1), in line with the results found for Nova et al.^{8d} Therefore, calculations have been carried out considering only the bidentate coordination mode of the phosphine ligand. Thus, initial binding of the naphthyl sulfamates to the active Pd(0) species generates η^2 -naphthyl sulfamate complex **A** located -4.3 kcal mol⁻¹ below the separate reactants in the free energy surface (Figure 2), which

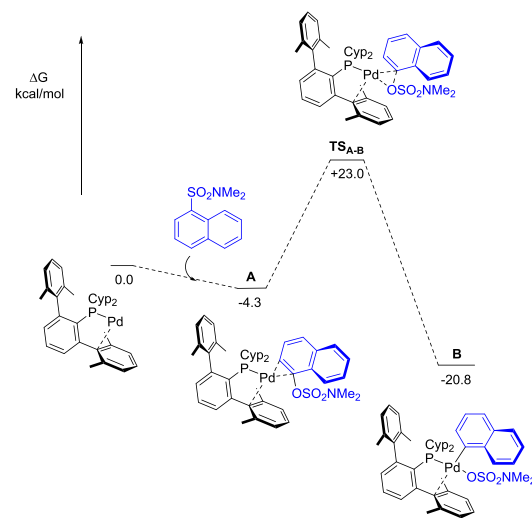


Figure 2. Gibbs free energy profile, in kcal mol⁻¹, for the oxidative addition step.

retains the bidentate coordination mode of the phosphine (k^1 -P, η^2 -C_{arene}). Subsequently, oxidative addition at **A** is exergonic by 16.5 kcal mol⁻¹ and gives rise to species **B** through an energy barrier of 27.3 kcal mol⁻¹. This barrier, which is only 1.8 kcal mol⁻¹ higher than that obtained by Nova et al.,^{8d} in combination with the energy gain for the formation of **B**, renders this step not reversible. In accordance with the results obtained by Nova et al., in the oxidative addition product **B**, the sulfamate and the phosphine ligands display mutual *trans* orientation. Only one of the sulphonyl oxygen atoms of the sulfamate is bonded to the metal (Pd–O = 2.224 Å), and the phosphine retained the bidentate coordination (k^1 -P, η^2 -C_{arene}), with the metrics for **B** being (Pd–C1' = 2.511 Å, Pd–C2' = 2.727 Å). To account for the lower reactivity observed for phenyl sulfamate derivatives, the oxidative addition of various *p*-substituted phenyl sulfamates (H, OH, CN) has been performed. Neutral or electron-donating substituents at the *p*-position of the aryl ring increase both the energy of the η^2 -sulfamate complex and the energy of the oxidative addition transition state, when compared with activated aryl sulfamates or naphthyl sulfamate (see Figure S2). This is consistent with our experimental observations.

For the ligand exchange step, first the oxidative addition intermediate **B** dissociates the sulfamate anion to give a T-shaped cationic complex **C**, where the position *trans* to the phosphine is vacant. This charge separation event is facilitated by polar solvents.²¹ In fact, calculations carried out with the continuum SMD model yielded energies of -19.8 and -26.1 kcal mol⁻¹ for separate **C** and sulfamate in ethanol and water, respectively. However, the same charge separation event calculated in toluene results in the separate fragments lying $+21.4$ kcal mol⁻¹ above the origin (Figure 3). These results support that polar protic solvent mixtures (ethanol and water)

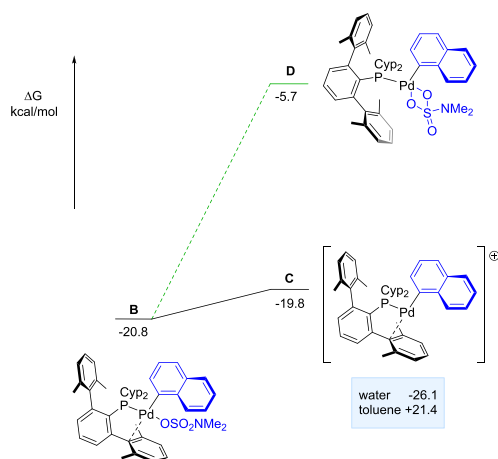


Figure 3. Energy profile of the evaluated pathways for ligand exchange stage. Gibbs free energy profiles are in kcal mol⁻¹.

favor a dissociative pathway involving the formation of cationic complex **C** with retention of the secondary interaction with the terphenyl moiety, in line with the experimental observations (see Table 1, entry 6).

Alternatively, the loss of the interaction between the metal and the flanking ring of the terphenyl substituent could also generate an open coordination site on the metal in intermediate **B**. However, the resulting species, **D**, which features k²-O coordination of the sulfamate is located 14.1 kcal mol⁻¹ higher in energy than **C** (Figure 3). While **D** may be an accessible intermediate at the temperature at which reaction occurs, this pathway fails to explain the effect of the polar solvent mixture *t*BuOH:H₂O in facilitating the reaction.

While aniline can coordinate to the metal center in the cationic intermediate **C** to yield the corresponding amino complex, other ligands present in the reaction mixture may also form intermediates worth considering in the analysis of the reaction mechanism (Figure 4). Consequently, we explored the coordination of aniline, water, OH⁻, and *t*BuO⁻.²²

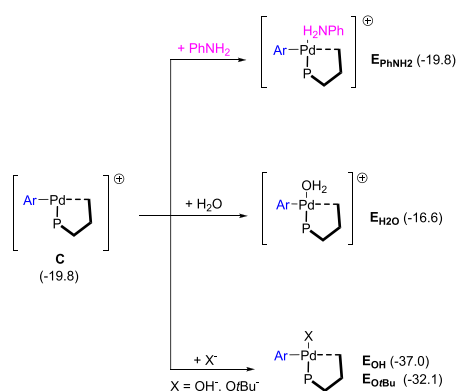


Figure 4. Reaction pathways evaluated for ligand coordination to **C**. In parenthesis: Gibbs energy in kcal mol⁻¹.

The coordination of aniline to **C** is thermoneutral (Figure 4), rendering cationic intermediate **E_{PhNH₂}**. Moreover, the association of H₂O to intermediate **C** (Figure 4) yields intermediate **E_{H₂O}** with a relative Gibbs energy of -16.6 kcal mol⁻¹, which is 3.2 kcal mol⁻¹ higher than that of the aniline adduct **E_{PhNH₂}**. Therefore, H₂O is not expected to be competitive with aniline for coordination to intermediate **C**.

However, OH⁻ coordinates to **C** to form neutral species **E_{OH}** located at -37.0 below the reactants (Figure 4). Similarly, *t*BuO⁻ forms a stable neutral adduct **E_{O*t*Bu}** but this species is present in very low concentrations (see below) in solution. The participation of the latter in the catalysis is deemed of little importance, and its discussion is relegated to the SI, while the role of the former is shown in the following paragraphs.

Following the above results, we envisioned two pathways for the ligand exchange step. The more favored one (shown in black in Figure 5) starts with cationic intermediate **E_{PhNH₂}**, which undergoes intermolecular deprotonation of the coordinated aniline by OH⁻. This step shows to be strongly favored thermodynamically ($\Delta G = -17.7$ kcal mol⁻¹), and importantly, the proton transfer occurs with a negligible energy barrier.²³ The resulting species **H**, which displays the anilido ligand in the *trans* position to phosphorus, has a relative Gibbs energy of -37.1 kcal mol⁻¹.

On the contrary, in the alternative pathway (shown in green in Figure 5), OH⁻ is acting as a ligand and as a base. From neutral intermediate **E_{OH}**, coordination of aniline delivers intermediate **F_{OH}**, located at -20.1 kcal mol⁻¹. Intramolecular deprotonation of aniline is endergonic and takes place through **TS_{FOH-GOH}**. The overall barrier from intermediate **E_{OH}** is 28.6 kcal mol⁻¹, slightly higher than that calculated for the oxidative step and higher than the reverse barrier for the dissociation of OH⁻ in **E_{OH}** to regenerate **C**. It is worth noting that all attempts to detect the corresponding Pd-hydroxo species experimentally were unsuccessful.

These considerations were further supported by application of microkinetic modeling. These analyses can give information about the evolution of the concentration of each species with time considering rate constants provided by DFT calculations.²⁴ In our case, the microkinetic model indicated that the calculated barrier for oxidative addition may be overestimated by ca. 2 kcal mol⁻¹ at 383 K and, more importantly, it revealed that **E_{H₂O}**, **E_{OH}**, and **E_{O*t*Bu}** were present in very low concentration in the reaction mixture during the catalysis (see Figures S3 and S4 in the Supporting Information). In addition, the microkinetic model verified that the contribution of any pathway other than the one starting from intermediate **E_{PhNH₂}** to the formation of the C–N coupling product is negligible.

Finally, the last stage of the catalytic cycle is the formation of the C–N bond from intermediate **H**. The reductive elimination takes place through **TS_{H-I}** (Figure 5) with an activation energy barrier of 11.9 kcal mol⁻¹, generating intermediate **I**, in which the C–N product is coordinated to the Pd(0) center through the N atom. To close the catalytic cycle, displacement of the diarylamine by naphthalen-1-yl dimethylsulfamate occurs with an energy cost of 2.25 kcal mol⁻¹.

CONCLUSIONS

In summary, we have developed a general Pd-based catalytic system for the amination of synthetically versatile aryl sulfamates. This protocol allows use of a broad range of *N*-nucleophiles including anilines, secondary amines, primary alkyl amines, heteroaryl amines, *N*-heterocycles, and primary amides. The use of a mixture of polar protic solvents (*t*BuOH:H₂O) has been found to be crucial to attaining high conversions. Computational studies show that oxidative addition of aryl sulfamate is the rate-limiting step and that in

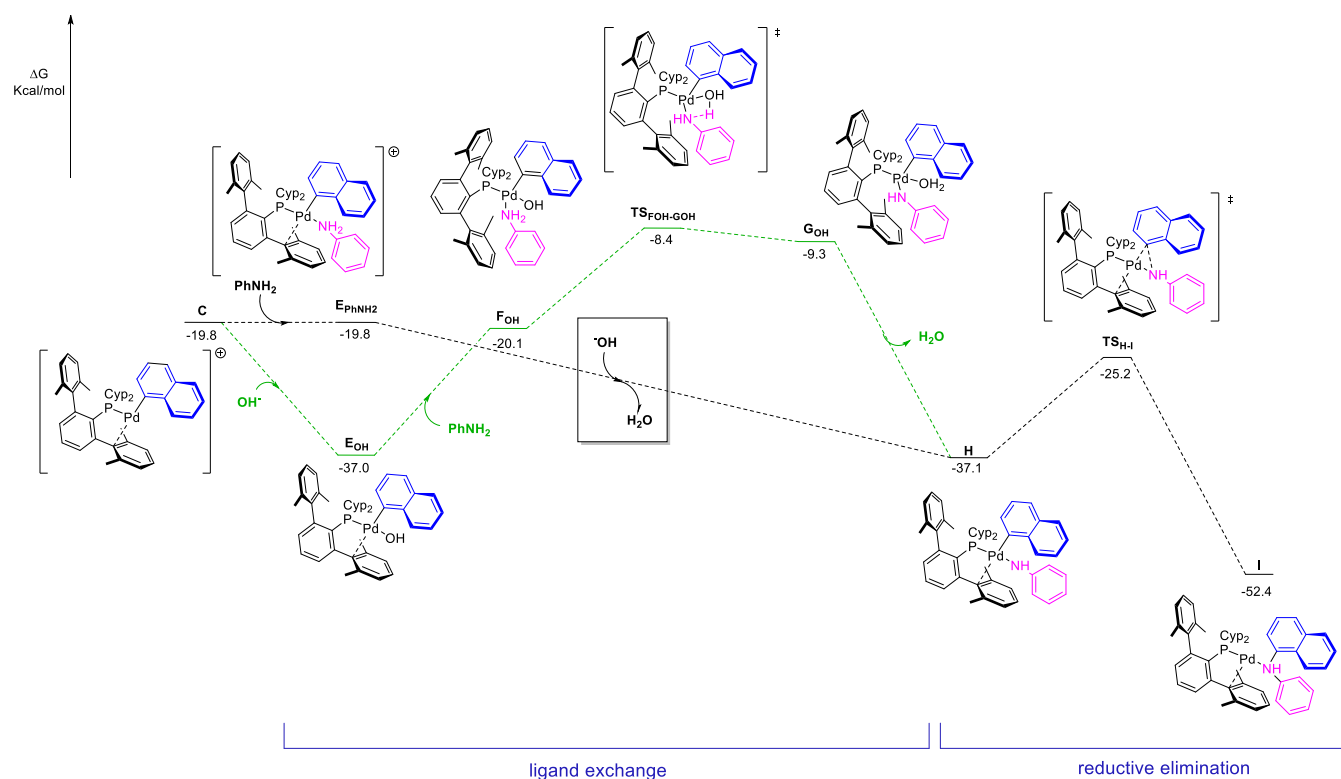


Figure 5. Energy profile of the proposed pathways for the ligand exchange step and reductive elimination. Gibbs energies are in kcal mol⁻¹.

polar protic solvents, the reaction proceeds through a cationic pathway.

ASSOCIATED CONTENT

Supporting Information

The Supporting Information is available free of charge at <https://pubs.acs.org/doi/10.1021/acscatal.3c03166>.

General considerations; optimization experiments; unsuccessful results with aryl sulfamates; synthesis of aryl sulfamate substrates; general catalytic procedures; characterization data of reaction products; NMR spectra of compounds; computational details; microkinetic model (PDF)

Optimized coordinates for calculated structures (XYZ)

AUTHOR INFORMATION

Corresponding Authors

Joaquín López-Serrano – Instituto de Investigaciones Químicas (IIQ), Departamento de Química Inorgánica and Centro de Innovación Química Avanzada (ORFEO-CINQA), Universidad de Sevilla and CSIC, 41092 Sevilla, Spain; orcid.org/0000-0003-3999-0155; Email: joaquin.lopez@iiq.csic.es

Auxiliadora Prieto – Laboratorio de Catálisis Homogénea, Unidad Asociada al CSIC, CIQSO-Centro de Investigación en Química Sostenible and Departamento de Química, Universidad de Huelva, 21007 Huelva, Spain; Email: maria.prieto@diq.uhu.es

M. Carmen Nicasio – Departamento de Química Inorgánica, Universidad de Sevilla, 41071 Sevilla, Spain; orcid.org/0000-0002-6485-2953; Email: mnicasio@us.es

Author

Andrea Monti – Departamento de Química Inorgánica, Universidad de Sevilla, 41071 Sevilla, Spain; orcid.org/0000-0002-4804-9909

Complete contact information is available at: <https://pubs.acs.org/10.1021/acscatal.3c03166>

Notes

The authors declare no competing financial interest.

ACKNOWLEDGMENTS

We thank financial support from MCIN/AEI/10.13039/501100011033 (Grant PID2020-113797RB-C22), US/JUNTA/FEDER, UE (Grant US-1262266), and FEDER, UE/Junta de Andalucía-Consejería de Transformación, Economía, e Industria, Conocimiento y Universidades (Grant P20_00624) for financial support. A.M. thanks MICINN for a research fellowship. A.P. thanks Ministerio de Universidades (Plan de Recuperación Transformación y Resiliencia) for financial support. The use of computational resources of the Universidad de Granada (cluster Albaicín) is thankfully acknowledged.

REFERENCES

- (1) (a) Qiu, Z.; Li, C.-J. Transformations of Less-Activated Phenols and Phenol Derivatives via C–O Cleavage. *Chem. Rev.* **2020**, *120*, 10454–10515. (b) Zeng, H.; Qiu, Z.; Domínguez-Huerta, A.; Hearne, Z.; Chen, Z.; Li, C.-J. An Adventure in Sustainable Cross-Coupling of Phenols and Derivatives via Carbon–Oxygen Bond Cleavage. *ACS Catal.* **2017**, *7*, 510–519. (c) Cornella, J.; Zarate, C.; Martín, R. Metal-catalyzed activation of ethers via C–O bond cleavage: a new strategy for molecular diversity. *Chem. Soc. Rev.* **2014**, *43*, 8081–8097.
- (2) For reviews see: (a) Rosen, B. M.; Quasdorf, K. W.; Wilson, D. A.; Zhang, N.; Resmerita, A.-M.; Garg, N. K.; Percec, V. Nickel-

Catalyzed Cross-Couplings Involving Carbon–Oxygen Bonds. *Chem. Rev.* **2011**, *111*, 1346–1416. (b) Tobisu, M.; Chatani, N. Cross-Couplings Using Aryl Ethers via C–O Bond Activation Enabled by Nickel Catalysts. *Acc. Chem. Res.* **2015**, *48*, 1717–1726. (c) Boit, T. B.; Bulger, A. S.; Dander, J. E.; Garg, N. K. Activation of C–O and C–N Bonds Using Non-Precious-Metal Catalysis. *ACS Catal.* **2020**, *10*, 12109–12126.

(3) For recent examples on Ni-catalyzed C–O bond activation see: (a) Lavoie, C. M.; MacQueen, P. M.; Rotta-Loria, N. L.; Sawatzky, R. S.; Borzenko, A.; Chisholm, A. J.; Hargreaves, B. K. V.; McDonald, R.; Ferguson, M. J.; Stradiotto, M. Challenging nickel-catalysed amine arylations enabled by tailored ancillary ligand design. *Nat. Commun.* **2016**, *7*, 11073. (b) MacQueen, P. M.; Tassone, J. P.; Diaz, C.; Stradiotto, M. Challenging nickel-catalysed amine arylations enabled by tailored ancillary ligand design. *J. Am. Chem. Soc.* **2018**, *140*, 5023–5027. (c) Zhang, J.; Sun, T.; Zhang, Z.; Cao, H.; Bai, Z.; Cao, Z.-C. Nickel-Catalyzed Enantioselective Arylative Activation of Aromatic C–O Bond. *J. Am. Chem. Soc.* **2021**, *143*, 18380–18387. (d) Borys, A. M.; Hevia, E. The Anionic Pathway in the Nickel-Catalysed Cross-Coupling of Aryl Ethers. *Angew. Chem., Int. Ed.* **2021**, *60*, 24659–24667. (e) Day, C. S.; Somerville, R. J.; Martin, R. Deciphering the dichotomy exerted by Zn(II) in the catalytic sp^2 C–O bond functionalization of aryl esters at the molecular level. *Nat. Catal.* **2021**, *4*, 124–133.

(4) For a review on Pd-catalyzed cross-coupling by C–O bond activation, see: Zhou, T.; Szostak, M. Palladium-catalyzed cross-couplings by C–O bond activation. *Catal. Sci. Technol.* **2020**, *10*, 5702–5739.

(5) (a) Snieckus, V. Directed Ortho Metalation. Tertiary Amide and O-Carbamate Directors in Synthetic Strategies for Polysubstituted Aromatics. *Chem. Rev.* **1990**, *90*, 879–933. (b) Macklin, T. K.; Snieckus, V. Directed Ortho Metalation Methodology. The *N,N*-Dialkyl Aryl *O*-Sulfamate as a New Directed Metalation Group and Cross-Coupling Partner for Grignard Reagents. *Org. Lett.* **2005**, *7*, 2519–2522. (c) Knappke, C. E. I.; von Wangelin, A. J. A Synthetic Double Punch: Suzuki–Miyaura Cross-Coupling Mates with C–H Functionalization. *Angew. Chem., Int. Ed.* **2010**, *49*, 3568–3570.

(6) (a) Bajo, S.; Laidlaw, G.; Kennedy, A. R.; Sproules, S.; Nelson, D. J. Oxidative Addition of Aryl Electrophiles to a Prototypical Nickel(0) Complex: Mechanism and Structure/Reactivity Relationships. *Organometallics* **2017**, *36*, 1662–1672. (b) Uthayopas, C.; Surawatanawong, P. Aryl C–O oxidative addition of phenol derivatives to nickel supported by an N-heterocyclic carbene via a Ni0 five-centered complex. *Dalton Trans.* **2019**, *48*, 7817–7827.

(7) (a) Rambren, S. D.; Silberstein, A. L.; Yang, Y.; Garg, N. K. Nickel-Catalyzed Amination of Aryl Sulfamates. *Angew. Chem., Int. Ed.* **2011**, *50*, 2171–2173. (b) Ackermann, L.; Sandmann, R.; Song, W. Palladium- and Nickel-Catalyzed Aminations of Aryl Imidazolylsulfonates and Sulfamates. *Org. Lett.* **2011**, *13*, 1784–1786. (c) Hie, L.; Ramgren, S. D.; Mesganaw, T.; Garg, N. K. Nickel-Catalyzed Amination of Aryl Sulfamates and Carbamates Using an Air-Stable Precatalyst. *Org. Lett.* **2012**, *14*, 4182–4185. (d) Nathel, N. F. F.; Kim, J.; Hie, L.; Jiang, X.; Garg, N. K. Nickel-Catalyzed Amination of Aryl Chlorides and Sulfamates in 2-Methyl-THF. *ACS Catal.* **2014**, *4*, 3289–3293. (e) Park, N. H.; Teverovskiy, G.; Buchwald, S. L. Development of an Air-Stable Nickel Precatalyst for the Amination of Aryl Chlorides, Sulfamates, Mesylates, and Triflates. *Org. Lett.* **2014**, *16*, 220–223. (f) Inaloo, I. D.; Majnooni, S.; Eslahi, H.; Esmailpour, M. N-Arylation of (hetero)arylamines using aryl sulfamates and carbamates via C–O bond activation enabled by a reusable and durable nickel(0) catalyst. *New J. Chem.* **2020**, *44*, 13266–13278.

(8) (a) Molander, G. A.; Shin, I. Pd-Catalyzed Suzuki–Miyaura Cross-Coupling Reactions between Sulfamates and Potassium Boc-Protected Aminomethyltrifluoroborates. *Org. Lett.* **2013**, *15*, 2534–2537. (b) Wang, Z.-Y.; Ma, Q.-N.; Li, R.-H.; Shao, L.-X. Palladium-catalyzed Suzuki–Miyaura coupling of aryl sulfamates with arylboronic acids. *Org. Biomol. Chem.* **2013**, *11*, 7899–7906. (c) Melvin, P. R.; Hazari, N.; Beromi, M. M.; Shah, H. P.; Williams, M. J. Pd-Catalyzed Suzuki–Miyaura and Hiyama–Denmark Couplings of Aryl

Sulfamates. *Org. Lett.* **2016**, *18*, 5784–5787. (d) Melvin, P. R.; Nova, A.; Balcells, D.; Hazari, N.; Tilset, M. DFT Investigation of Suzuki–Miyaura Reactions with Aryl Sulfamates Using a Dialkylbiarylphosphine-Ligated Palladium Catalyst. *Organometallics* **2017**, *36*, 3664–3675.

(9) (a) Marín, M.; Moreno, J. J.; Navarro-Gilabert, C.; Álvarez, E.; Maya, C.; Peloso, R.; Nicasio, M. C.; Carmona, E. Synthesis, Structure and Nickel Carbonyl Complexes of Dialkylterphenyl Phosphines. *Chem. – Eur. J.* **2019**, *25*, 260–272. (b) Marín, M.; Moreno, J. J.; Alcaide, M. M.; Álvarez, E.; López-Serrano, J.; Campos, J.; Nicasio, M. C.; Carmona, E. Evaluating Stereoelectronic Properties of Bulky Dialkylterphenyl Phosphine Ligands. *J. Organomet. Chem.* **2019**, *896*, 120–128.

(10) (a) Moreno, J. J.; Espada, M. F.; Campos, J.; López-Serrano, J.; Macgregor, S. A.; Carmona, E. Base-Promoted, Remote C–H Activation at a Cationic (η^5 -C₅Me₅)Ir(III) Center Involving Reversible C–C Bond Formation of Bound C₅Me₅. *J. Am. Chem. Soc.* **2019**, *141*, 2205–2210. (b) Martín, M. T.; Marín, M.; Rama, R. J.; Álvarez, E.; Maya, C.; Molina, F.; Nicasio, M. C. Zero-valent ML₂ complexes of group 10 metals supported by terphenyl phosphanes. *Chem. Commun.* **2021**, *57*, 3083–3086.

(11) (a) Rama, R. J.; Maya, C.; Nicasio, M. C. Dialkylterphenyl Phosphine-Based Palladium Precatalysts for Efficient Aryl Amination of *N*-Nucleophiles. *Chem. – Eur. J.* **2020**, *26*, 1064–1073. (b) Monti, A.; Rama, R. J.; Gómez, B.; Maya, C.; Alvarez, E.; Carmona, E.; Nicasio, M. C. *N*-substituted aminobiphenyl palladacycles stabilized by dialkylterphenyl phosphanes: Preparation and applications in C–N cross-coupling reactions. *Inorg. Chim. Acta* **2021**, *518*, No. 120214.

(12) (a) Ruiz-Castillo, P.; Buchwald, S. L. Applications of Palladium-Catalyzed C–N Cross-Coupling Reactions. *Chem. Rev.* **2016**, *116*, 12564–12649. (b) Dorel, R.; Grugel, C. P.; Haydl, A. M. The Buchwald–Hartwig Amination After 25 Years. *Angew. Chem., Int. Ed.* **2019**, *58*, 17118–17129. (c) Rayadurgam, J.; Sana, S.; Sasikummar, M.; Gu, Q. Development of an Air-Stable Nickel Precatalyst for the Amination of Aryl Chlorides, Sulfamates, Mesylates, and Triflates. *Org. Chem. Front.* **2020**, *8*, 384–414.

(13) Rama, R. J.; Maya, C.; Molina, F.; Nova, A.; Nicasio, M. C. Important Role of NH-Carbazole in Aryl Amination Reactions Catalyzed by 2-Aminobiphenyl Palladacycles. *ACS Catal.* **2023**, *13*, 3934–3948.

(14) See for example: (a) Huang, X.; Anderson, K. W.; Zim, D.; Jiang, L.; Klapars, A.; Buchwald, S. L. Expanding Pd-Catalyzed C–N Bond-Forming Processes: The First Amidation of Aryl Sulfonates, Aqueous Amination, and Complementarity with Cu-Catalyzed Reactions. *J. Am. Chem. Soc.* **2003**, *125*, 6653–6655. (b) Fors, B. P.; Dooleweerd, K.; Zeng, Q.; Buchwald, S. L. An Efficient System for the Pd-Catalyzed Cross-Coupling of Amides and Aryl Chlorides. *Tetrahedron* **2009**, *65*, 6576–6583.

(15) (a) Kuwano, R.; Utsunomiya, M.; Hartwig, J. F. Aqueous Hydroxide as a Base for Palladium-Catalyzed Amination of Aryl Chlorides and Bromides. *J. Org. Chem.* **2002**, *67*, 6479–6486. (b) Dallas, A. S.; Gothelf, K. V. Effect of Water on the Palladium-Catalyzed Amidation of Aryl Bromides. *J. Org. Chem.* **2005**, *70*, 3321–3323. (c) Lau, S.-H.; Yu, P.; Chen, L.; Madsen-Duggan, C. B.; Williams, M. J.; Carrow, B. P. Aryl Amination Using Soluble Weak Base Enabled by a Water-Assisted Mechanism. *J. Am. Chem. Soc.* **2020**, *142*, 20030–20039.

(16) (a) Magano, J.; Dunetz, J. Large-Scale Applications of Transition Metal-Catalyzed Couplings for the Synthesis of Pharmaceuticals. *Chem. Rev.* **2011**, *111*, 2177–2250. (b) McGowan, M. A.; Henderson, J. L.; Buchwald, S. L. Palladium-Catalyzed *N*-Arylation of 2-Aminothiazoles. *Org. Lett.* **2012**, *14*, 1432–1435.

(17) Fujita, K.; Yamashita, M.; Puschmann, F.; Alvarez-Falcon, M. M.; Incarvito, C. D.; Hartwig, J. F. Organometallic Chemistry of Amidate Complexes. Accelerating Effect of Bidentate Ligands on the Reductive Elimination of *N*-Aryl Amidates from Palladium(II). *J. Am. Chem. Soc.* **2006**, *128*, 9044–9045.

(18) (a) Yin, J.; Buchwald, S. L. Pd-Catalyzed Intermolecular Amidation of Aryl Halides: The Discovery that Xantphos Can Be

Trans-Chelating in a Palladium Complex. *J. Am. Chem. Soc.* **2002**, *124*, 6043–6048. (b) Klapars, A.; Campos, K. R.; Chen, C.-Y.; Volante, R. P. Preparation of Enamides via Palladium-Catalyzed Amidation of Enol Tosylates. *Org. Lett.* **2005**, *7*, 1185–1188. (c) Dooleweerd, K.; Fors, B. P.; Buchwald, S. L. Pd-Catalyzed Cross-Coupling Reactions of Amides and Aryl Mesylates. *Org. Lett.* **2010**, *12*, 2350–2353.

(19) Lavoie, C. M.; MacQueen, P. M.; Stradiotto, M. Nickel-Catalyzed N-Arylation of Primary Amides and Lactams with Activated (Hetero)aryl Electrophiles. *Chem. – Eur. J.* **2016**, *22*, 18752–18755.

(20) (a) Lombardi, C.; Rucker, R. P.; Froese, R. D. J.; Sharif, S.; Champagne, P. A.; Organ, M. G. Rate and Computational Studies for Pd-NHC-Catalyzed Amination with Primary Alkylamines and Secondary Anilines: Rationalizing Selectivity for Monoarylation versus Diarylation with NHC Ligands. *Chem. – Eur. J.* **2019**, *25*, 14223–14229. (b) Sunesson, Y.; Limé, E.; Lill, S. O. N.; Meadows, R. E.; Norrby, P.-O. Role of the Base in Buchwald–Hartwig Amination. *J. Org. Chem.* **2014**, *79*, 11961–11969. (c) Hoi, K. H.; Çalimsiz, S.; Froese, R. D. J.; Hopkinson, A. C.; Organ, M. G. Amination with Pd–NHC Complexes: Rate and Computational Studies on the Effects of the Oxidative Addition Partner. *Chem. – Eur. J.* **2011**, *17*, 3086–3090.

(d) Hoi, K. H.; Çalimsiz, S.; Froese, R. D. J.; Hopkinson, A. C.; Organ, M. G. Amination with Pd–NHC Complexes: Rate and Computational Studies Involving Substituted Aniline Substrates. *Chem. – Eur. J.* **2012**, *18*, 145–151. (e) Cundari, T. R.; Deng, J. Density Functional Theory Study of Palladium-Catalyzed Aryl–Nitrogen and Aryl–Oxygen Bond Formation. *J. Phys. Org. Chem.* **2005**, *18*, 417–425. (f) McMullin, C. L.; Rühle, B.; Besora, M.; Orpen, A. G.; Harvey, J. N.; Fey, N. Computational Study of PtBu₃ as Ligand in the Palladium-Catalyzed Amination of Phenylbromide with Morpholine. *J. Mol. Catal. A: Chem.* **2010**, *324*, 48–55. (g) Yong, F. F.; Mak, A. M.; Wu, W.; Sullivan, M. B.; Robins, E. G.; Johannes, C. W.; Jong, H.; Lim, Y. H. Empirical and Computational Insights into N-Arylation Reactions Catalyzed by Palladium Meta-Terarylphosphine Catalyst. *Chempluschem* **2017**, *82*, 750–757. (h) Kim, S.-T.; Pudasaini, B.; Baik, M.-H. Mechanism of Palladium-Catalyzed C–N Coupling with 1,8-Diazabicyclo[5.4.0]Undec-7-Ene (DBU) as a Base. *ACS Catal.* **2019**, *9*, 6851–6856. (i) Gómez-Orellana, P.; Lledós, A.; Ujaque, G. Computational Analysis on the Pd-Catalyzed C–N Coupling of Ammonia with Aryl Bromides Using a Chelate Phosphine Ligand. *J. Org. Chem.* **2021**, *86*, 4007–4017. (j) Ikawa, T.; Barder, T. E.; Biscoe, M. R.; Buchwald, S. L. Pd-Catalyzed Amidation of Aryl Chlorides Using Monodentate Biaryl Phosphine Ligands: A Kinetic, Computational, and Synthetic Investigation. *J. Am. Chem. Soc.* **2007**, *129*, 13001–13007. (k) Barder, T. E.; Buchwald, S. L. Insights into Amine Binding to Biaryl Phosphine Palladium Oxidative Addition Complexes and Reductive Elimination from Biaryl Phosphine Arylpalladium Amido Complexes via Density Functional Theory. *J. Am. Chem. Soc.* **2007**, *129*, 12003–12010.

(21) Jutand, A.; Mosleh, A. Rate and Mechanism of Oxidative Addition of Aryl Triflates to Zerovalent Palladium Complexes. Evidence for the Formation of Cationic (σ -Aryl)palladium Complexes. *Organometallics* **1995**, *14*, 1810–1817.

(22) McMullin, C. L.; Jover, J.; Harvey, J. N.; Fey, N. Accurate modelling of Pd(0) + PhX oxidative addition kinetics. *Dalton Trans.* **2010**, *39*, 10833–10836.

(23) Intermolecular deprotonation of EtNH₂ shows an energy barrier of 2 kcal mol⁻¹, see SI for details.

(24) (a) Besora, M.; Maseras, F. Microkinetic Modeling in Homogeneous Catalysis. *WIREs Comput. Mol. Sci.* **2018**, *8*, No. e1372. (b) Jaraiz, M. DFT-Based Microkinetic Simulations: A Bridge Between Experiment and Theory in Synthetic Chemistry. In *Topics in Organometallic Chemistry*; Springer Science and Business Media Deutschland GmbH, 2020; Vol. 67, pp. 81–105.

Recommended by ACS

Leveraging the Redox Promiscuity of Nickel To Catalyze C–N Coupling Reactions

Olivia R. Taylor, Ana Bahamonde, *et al.*

JANUARY 17, 2024

THE JOURNAL OF ORGANIC CHEMISTRY

READ 

Computational Methods Enable the Prediction of Improved Catalysts for Nickel-Catalyzed Cross-Electrophile Coupling

Michelle E. Akana, Daniel J. Weix, *et al.*

JANUARY 26, 2024

JOURNAL OF THE AMERICAN CHEMICAL SOCIETY

READ 

Ligand-Enabled *ortho*-Arylation of (hetero)Aromatic Acids with 2,6-Disubstituted Aryl Halides

Xianglin Luo, Liangbin Huang, *et al.*

AUGUST 30, 2023

ACS CATALYSIS

READ 

W-Phos Ligand Enables Copper-Catalyzed Enantioselective Alkylation of *N*-Sulfonyl Ketimines with Grignard Reagents

Li-Ming Zhang, Junliang Zhang, *et al.*

JUNE 20, 2023

ACS CATALYSIS

READ 

Get More Suggestions >